Multipolar tensor analysis of second-order nonlinear optical response of surface and bulk of glass

Francisco J. Rodríguez[*]**, Fu Xiang Wang, Brian K. Canfield, Stefano Cattaneo**[1]**, and Martti Kauranen**

Institute of Physics, Tampere University of Technology, P.O.Box 692, FI-33101 Tampere, Finland
[1]Current address: Philips Research, High Tech Campus 34 (MS 41), 5656 AE Eindhoven, The Netherlands
[*]Corresponding author: francisco.rodriguezmartinez@tut.fi

Abstract: We use two-beam second-harmonic generation to perform a quantitative tensor analysis of the effective dipolar surface nonlinearity and the separable multipolar bulk nonlinearity for BK7 glass. The most straightforward, self-consistent interpretation of the results is obtained when the effective surface response is assumed to have approximate Kleinman symmetry and the bulk contribution is dominated by magnetic, rather than quadrupole, effects.

©2007 Optical Society of America

OCIS codes: (190.4350) Nonlinear optics at surfaces; (160.2750) Glass and other amorphous materials.

References and links

1. Y. R. Shen, *The Principles of Nonlinear Optics* (Wiley, New York, 1984).
2. P. Guyot-Sionnest, W. Chen, Y. R. Shen, "General considerations on optical second-harmonic generation from surfaces and interfaces," Phys. Rev. B **33**, 8254-8263 (1986).
3. N. Bloembergen, R. K. Chang, S. S. Jha, C. H. Lee, "Optical Second-Harmonic Generation in Reflection from Media with Inversion Symmetry," Phys. Rev. **174**, 813-822 (1968).
4. J. E. Sipe, V. Mizrahi, G. I. Stegeman, "Fundamental difficulty in the use of 2nd-harmonic generation as a strictly surface probe," Phys. Rev. B **35**, 9091-9094 (1987).
5. P. Guyot-Sionnest and Y. R. Shen, "Local and nonlocal surface nonlinearities for surface optical 2nd-harmonic generation," Phys. Rev. B **35**, 4420-4426 (1987).
6. P. Guyot-Sionnest and Y. R. Shen, "Bulk contribution in surface 2nd-harmonic generation," Phys. Rev. B **38**, 7985-7989 (1988).
7. Y. R. Shen, "Surface contribution versus bulk contribution in surface nonlinear optical spectroscopy," Appl. Phys. B:Lasers Opt. **68**, 295-300 (1999).
8. X. Wei, S.-C. Hong, A. I. Lvovsky, H. Held, Y. R. Shen, "Evaluation of surface vs bulk contributions in sum-frequency vibrational spectroscopy using reflection and transmission geometries," J. Phys. Chem. B **104**, 3349-3354 (2000).
9. H. Held, A. I. Lvovsky, X. Wei, Y. R. Shen, "Bulk contribution from isotropic media in surface sum-frequency generation," Phys. Rev. B **66**, 205110 (2002).
10. S. Cattaneo and M. Kauranen, "Polarization-based identification of bulk contributions in surface nonlinear optics," Phys. Rev. B **72**, 033412 (2005).
11. S. Cattaneo and M. Kauranen, "Bulk versus surface contributions in nonlinear optics of isotropic centrosymmetric media," Phys. Status Solidi B **242**, 3007-3011 (2005).
12. L. Sun, P. Figliozzi, Y. Q. An, M. C. Downer, W. L. Mochán, B. S. Mendoza, "Nonresonant quadrupolar second-harmonic generation in isotropic solids by use of two orthogonally polarized laser beams," Opt. Lett. **30**, 2287-2289 (2005).
13. P. Figliozzi, L. Sun, Y. Jiang, N. Matlis, B. Mattern, M. C. Downer, S. P. Withrow, C. W. White, W. L. Mochán, B. S. Mendoza, "Single-beam and enhanced two-beam second-harmonic generation from silicon nanocrystals by use of spatially inhomogeneous femtosecond pulses," Phys. Rev. Lett. **94**, 047401 (2005).
14. B. Koopmans, "Separation Problems in Optical Spectroscopies," Phys. Scr. **T109**, 80-88 (2004).
15. B. Koopmans, *Interface and Bulk Contributions in Optical Second-Harmonic Generation* (Ph.D. thesis, University of Groningen, 1993).
16. S. Cattaneo, *Two-Beam Surface Second-Harmonic Generation* (Ph.D. thesis, Tampere University of Technology, 2004).

17. J. E. Sipe, "New green-function formalism for surface optics," J. Opt. Soc. Am. B **4**, 481-489 (1987).
18. T. F. Heinz, "Second-order nonlinear optical effects at surfaces and interfaces," in *Nonlinear Surface Electromagnetic Phenomena*, H. E. Ponath and G. I. Stegeman, eds. (Elsevier, Amsterdam, 1991), pp. 353-416.
19. S. Cattaneo, M. Siltanen, F. X. Wang, M. Kauranen, "Suppression of nonlinear optical signals in finite interaction volumes of bulk materials," Opt. Express. **13**, 9714-9720 (2005).
20. S. Cattaneo, E. Vuorimaa, H. Lemmetyinen, M. Kauranen, "Advantages of polarized two-beam second-harmonic generation in precise characterization of thin films," J. Chem. Phys. **120**, 9245-9252 (2004).
21. W. Zhang, D. Zheng, Y. Xu, H. Bian, Y. Guo, H. Wang, "Reconsideration of second-harmonic generation from isotropic liquid interface: Broken Kleinman symmetry of neat air/water interface from dipolar contribution," J. Chem. Phys. **123**, 224713 (2005).
22. R. W. Boyd, *Nonlinear Optics* (Academic Press, San Diego, 2003).
23. M. Wohlfahrt, P. Strehlow, C. Enss, S. Hunklinger, "Magnetic-field effects in non-magnetic glasses," Europhys. Lett. **56**, 690-694 (2001).
24. B. Koopmans, A. M. Janner, H. T. Jonkman, G. A. Sawatzky, F. van der Woude, "Strong bulk magnetic dipole induced second-harmonic generation from C-60," Phys. Rev. Lett. **71**, 3569-3572 (1993).
25. S. L. Oliveira, S. C. Rand, "Intense nonlinear magnetic dipole radiation at optical frequencies: molecular scattering in a dielectric liquid," Phys. Rev. Lett. **98**, 093901 (2007).

1. Introduction

Second-order nonlinear optical processes, such as second-harmonic generation (SHG) and sum-frequency generation (SFG) are only allowed in noncentrosymmetric materials within the electric-dipole approximation of the light-matter interaction. Thus, a medium with inversion symmetry cannot generate second-order signals in its bulk. The inversion symmetry is always broken at the surface of the medium, and second-order effects can occur in a thin transition layer in which the material properties or the electromagnetic fields are modified [1,2]. This property allows second-order techniques to be used as highly sensitive probes of surfaces and interfaces.

When magnetic-dipole and electric-quadrupole interactions are considered, however, second-order processes can occur even in the bulk of centrosymmetric materials [2-4]. Such multipole interactions are usually much weaker than the electric-dipole interaction. On the other hand, multipole signals can grow over large portions of the bulk material and thereby reach a final magnitude comparable to the surface signal. For surface and interface probes, it is important to be able to distinguish between the surface and bulk signals. From a different point of view, materials with strong multipolar effects could lead to new nonlinear materials without the noncentrosymmetry limitation.

In addition to the electric-dipole contribution that arises from the non-centrosymmetry of the surface, there are quadrupolar contributions to the surface nonlinearity due to strong field and material gradients at the boundary between two media. These quadrupolar contributions behave like the dipole contribution and are included in an effective dipolar surface susceptibility [2,5,6]. Furthermore, the bulk response includes two parts. One of them cannot be separated from the surface response and is therefore also added to the measured surface susceptibility [4]. The other can be measured in proper experiments and is known as the separable bulk contribution.

The distinction between the effective surface contribution and the separable bulk contribution has been a long-standing problem in surface nonlinear optics [7-9]. Traditional attempts have been based on differences between the coherence lengths of the reflected and transmitted bulk signals, which requires absolute calibration of the two signals and complicated experiments, or on different SFG spectra of the surface and bulk, which is limited to specific surface systems. Recently, the two contributions have been separated in an unambiguous and quantitative way by relying on their different polarization properties [10,11]. The possibility for unambiguous separation also opens the door for the search of new, multipolar nonlinear materials [12,13].

The role of multipole contributions to the nonlinear response of the surface and bulk of various materials is still not well understood. Qualitative arguments have been used to estimate the importance of contributions that cannot be directly measured, but their validity is

questionable. For example, the magnitude of the separable bulk contribution has been used as a measure of the importance of the bulk contribution to the effective surface response. However, depending on the dominant multipolar mechanism, even the relative sign of the two contributions can be different [14-16], thereby allowing any ratio between the two contributions when several mechanisms are active.

In this paper, we present a detailed and quantitative multipolar tensor analysis of the surface and bulk SHG from transparent BK7 glass. The effective surface nonlinearity and the separable bulk nonlinearity are both found to contribute significantly. The most straightforward self-consistent interpretation of the results suggests, surprisingly, that the bulk response has predominantly magnetic-dipole, rather than quadrupolar origin.

2. Theoretical background

The geometry for two-beam SHG is shown in Fig. 1. We take the z axis perpendicular to the surface of the sample and the y axis perpendicular to the plane of incidence. We denote quantities at the fundamental frequency (ω) with lower-case letters and those at the second harmonic frequency (2ω) with upper-case letters.
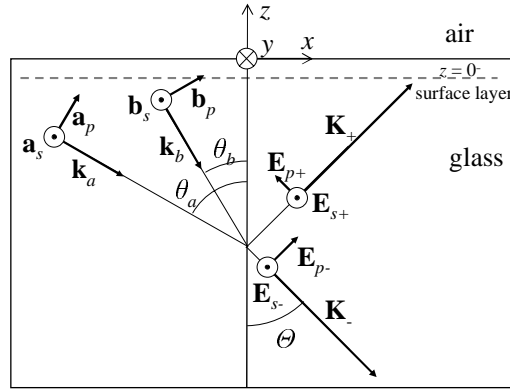

Fig. 1. Fields inside the nonlinear material in a two-beam SHG configuration.

We consider two plane waves at the fundamental frequency incident from air and superposed on the sample. The total fundamental field at point $\mathbf{r}$ inside the material is thus

$$\mathbf{e}(\mathbf{r}) = \mathbf{a}(\mathbf{r}) + \mathbf{b}(\mathbf{r}) = \mathbf{a}e^{i\mathbf{k}_a \cdot \mathbf{r}} + \mathbf{b}e^{i\mathbf{k}_b \cdot \mathbf{r}} , \qquad (1)$$

where $\mathbf{k}_a$ and $\mathbf{k}_b$ are the wavevectors and $\mathbf{a}$ and $\mathbf{b}$ are the complex electric-field amplitudes of the beams. Compared to incident fields from air, the field amplitudes $\mathbf{a}$ and $\mathbf{b}$ must therefore be corrected by the Fresnel transmission coefficients from air to glass, and the incidence angles θ_a and θ_b by Snell's law.

The fundamental beams give rise to nonlinear sources in the medium at the second-harmonic frequency. The sources radiate both in the forward (negative z, $\mathbf{E}_-e^{i\mathbf{K}_- \cdot \mathbf{r}}$) and backward (positive z, $\mathbf{E}_+e^{i\mathbf{K}_+ \cdot \mathbf{r}}$) directions, with fields also evaluated in the material. The propagation angle Θ of the SHG beams is obtained from momentum (wave vector) conservation along the surface [17]: $N\sin\Theta = n(\sin\theta_a + \sin\theta_b)/2$, where n (N) is the refractive index at ω (2ω). The phase mismatch $\Delta\mathbf{k}_\pm = \mathbf{k}_a + \mathbf{k}_b - \mathbf{K}_\pm$ therefore points along the z direction and we will denote $\Delta k_\pm = w_a + w_b \pm W$, with $W = 2\omega N\cos\Theta/c$ and $w_{a,b} = \omega n\cos\theta_{a,b}/c$, where c is the speed of light.

We model the effective surface contribution as an infinitely thin polarization sheet just inside the material, driven by the fields also just inside (Fig. 1). The response in which both fundamental beams contribute can be described by a polarization

$$\mathbf{P}^{sf}(z=0^-) = 2\boldsymbol{\chi}^{sf} : \mathbf{a}(z=0^-)\mathbf{b}(z=0^-),\qquad(2)$$

where $\boldsymbol{\chi}^{sf}$ is the effective surface susceptibility including both dipolar and multipolar contributions [2,5]. For isotropic surfaces ($C_{\infty v}$ symmetry), the susceptibility has three independent components [2]: $\chi^{sf}_{zxx} = \chi^{sf}_{zyy}$, $\chi^{sf}_{xxz} = \chi^{sf}_{xzx} = \chi^{sf}_{yyz} = \chi^{sf}_{yzy}$ and χ^{sf}_{zzz}. As a result, the components of the source polarization are:

$$P^{sf}_x = 2\chi^{sf}_{xxz}(a_x b_z + a_z b_x)$$
$$P^{sf}_y = 2\chi^{sf}_{xxz}(a_y b_z + a_z b_y)\qquad(3)$$
$$P^{sf}_z = 2\chi^{sf}_{zzz}a_z b_z + 2\chi^{sf}_{zxx}(a_x b_x + a_y b_y).$$

The projection of the sources along the *s* and *p* directions of the forward (-) and backward (+) SHG signals, with the fields of the incident beams also expressed in their respective *s* and *p* components (see Fig. 1) yields the following results:

$$P^{sf}_{s\pm} = 2\chi^{sf}_{xxz}(\sin\theta_a a_p b_s + \sin\theta_b a_s b_p)$$
$$P^{sf}_{p\pm} = 2(\mp\chi^{sf}_{xxz}\sin(\theta_a + \theta_b)\cos\Theta + \chi^{sf}_{zxx}\cos\theta_a\cos\theta_b\sin\Theta\qquad(4)$$
$$+ \chi^{sf}_{zzz}\sin\theta_a\sin\theta_b\sin\Theta)a_p b_p + 2\chi^{sf}_{zxx}\sin\Theta a_s b_s.$$

The SHG fields resulting from this polarization sheet are then [17]

$$\mathbf{E}^{sf}_\pm = i\frac{8\pi\omega^2}{Wc^2}\mathbf{P}^{sf}_\pm.\qquad(5)$$

When calculating the total second-harmonic field in the forward direction, we also take into account the backward-generated field reflected by the front surface. The total field inside the material is then $E^{sf}_{j-} + R_j E^{sf}_{j+}$ where $j = s,p$ and R_j is the Fresnel reflection coefficient from the glass-air interface at the second-harmonic frequency. The measured signal fields after the sample are further obtained by accounting for the Fresnel transmission coefficients from glass into air.

The bulk response of an isotropic material is described by the effective polarization [2-4]:

$$\mathbf{P}^{bulk}(\mathbf{r}) = \beta\,\mathbf{e}(\mathbf{r})[\nabla\cdot\mathbf{e}(\mathbf{r})] + \gamma\,\nabla[\mathbf{e}(\mathbf{r})\cdot\mathbf{e}(\mathbf{r})] + \delta'[\mathbf{e}(\mathbf{r})\cdot\nabla]\mathbf{e}(\mathbf{r}),\qquad(6)$$

where β, γ, and δ' are material parameters determined by the electric-quadrupole and magnetic-dipole tensors [14-16]. For homogeneous media $\nabla\cdot\mathbf{e}(\mathbf{r}) = 0$ and the first term vanishes. The second term is indistinguishable from the surface contribution as long as the surface is not modified. Its contribution can be included in the effective surface susceptibility by redefining its tensor components as $\chi_{zzz} = \chi^{sf}_{zzz} + \gamma$ and $\chi_{zxx} = \chi^{sf}_{zxx} + \gamma$. The third term is the separable bulk contribution. It will be nonzero only when the material interacts with two noncollinear beams. Thus, δ' is the only measurable bulk parameter [4,6,18].

In our geometry, the separable bulk contribution becomes:

$$\mathbf{P}^\delta(\mathbf{r}) = \delta'[\mathbf{e}(\mathbf{r})\cdot\nabla]\mathbf{e}(\mathbf{r}) = i\delta'((\mathbf{b}\cdot\mathbf{k}_a)\mathbf{a} + (\mathbf{a}\cdot\mathbf{k}_b)\mathbf{b})e^{i(\mathbf{k}_a+\mathbf{k}_b)\cdot\mathbf{r}}.\qquad(7)$$

The projection of this source along the *s* and *p* directions of the forward (-) and backward (+) SHG yields:

$$P^\delta_{s\pm} = i\delta' k\sin(\theta_a - \theta_b)(a_s b_p - a_p b_s)$$
$$P^\delta_{p\pm} = i\delta' k\sin(\theta_a - \theta_b)((\sin\theta_a - \sin\theta_b)\sin\Theta \mp (\cos\theta_a - \cos\theta_b)\cos\Theta)a_p b_p,\qquad(8)$$

where $k = \omega n/c$.

To calculate the SHG fields generated by the bulk source, we need to integrate over the finite overlap of the two input beams. In the practical limit where the length of the overlap region is much larger than the coherence length $l_c = \pi/|\Delta k|$, the signals are essentially suppressed when the whole interaction volume is located inside the bulk [12,19]. On the other hand, the bulk signals are maximized when the maximum overlap is located at a surface.

When the overlap is centered at the front surface and the material extends beyond the end of the overlap, the SHG amplitude can be approximated to very good accuracy as [11,19]:

$$\mathbf{E}_{\pm}^{\delta} \approx \frac{-8\pi\omega^2}{Wc^2\Delta k_{\pm}}\mathbf{P}_{\pm}^{\delta} \,. \tag{9}$$

We note that this result does not depend on the detailed shape of the overlap region. The total amplitude of the second-harmonic signal in transmission is again calculated by taking into account the backward-generated field reflected by the front surface and transmitted out of the sample through the back surface.

Comparing Eqs. (4) and (8), we see that both the surface and bulk contributions have the same functional dependence on the fundamental fields. The total measured SHG field, including both contributions, is therefore of the form:

$$\begin{aligned}
E_p &= f_p a_p b_p + g_p a_s b_s \\
E_s &= h_s a_p b_s + k_s a_s b_p \,,
\end{aligned} \tag{10}$$

where f_p, g_p, h_s, and k_s are experimental coefficients that depend on the surface and bulk parameters of the material and also on the experimental geometry and whose expressions can be deduced from Eqs. (4) and (8). Their relative values can be determined by measuring the SHG intensity for different combinations of the polarizations of the fundamental and SHG beams [20]. We then use the measured values of the coefficients and their theoretical expressions to obtain the relative values of the quantities $\chi_{zzz}^{sf} + \gamma$, $\chi_{zxx}^{sf} + \gamma$, χ_{xxz}^{sf}, and δ'.

3. Experimental results

In our experiments (Fig. 2), light from a Q-switched Nd:YAG laser (1064 nm, 20 mJ, 10 ns, 30 Hz) was split into two beams of approximately the same intensity. The polarization of the first beam was kept always linear, but a number of different polarization angles with respect to the plane of incidence were used. The polarization of the second beam, initially parallel to the plane of incidence, was varied with a rotating quarter-wave plate. The beams were made to intersect in the front surface of a 5 mm thick BK7 glass plate with incidence angles of 37° and 55° respectively. The diameter of the beams at the sample was approximately 0.5 mm. The second harmonic light (532 nm) generated jointly by the two beams in the glass sample was detected in transmission with a photomultiplier tube. A polarizer was placed before the photomultiplier tube in order to detect different fixed polarization components of the SHG light. The index of refraction of BK7 glass is n(1064 nm) = 1.507 and N(532 nm) = 1.519. With these parameters, we estimate that the beam overlap is 8 mm long and the coherence lengths are 0.1 µm (reflection) and 14 µm (transmission), thereby justifying the approximations behind Eq. (9).
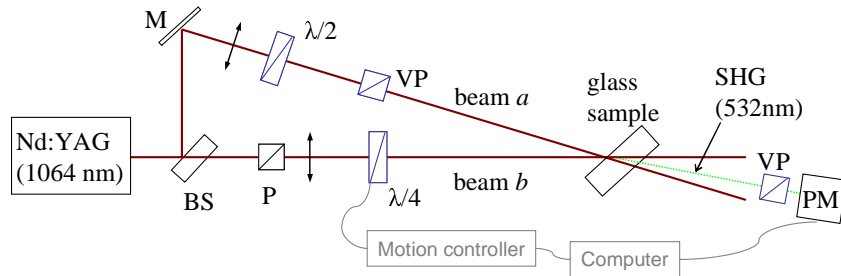
Fig. 2. Experimental setup for two-beam second-harmonic generation. BP, beam splitter; M, mirror; P, polarizer; VP, variable-angle polarizers; PM, photomultiplier tube. The linear polarization of the fundamental beam *a* is chosen with a variable-angle polarizer. The polarization of the second fundamental beam *b*, initially parallel to the plane of incidence, was varied with a rotating quarter-wave plate. The linear polarization of the detected SHG light is also chosen with a variable-angle polarizer.

We measured the SHG intensity as a function of the angle of rotation of the quarter-wave plate for different combinations of the fixed polarizations. In particular, we used the combinations 45° (*s*), 45° (*p*), *p* (45°) and *s* (45°) for the fixed fundamental (SHG) polarizations. The results were fitted with Eq. (10) in order to obtain the relative values of the experimental parameters f_p, g_p, h_s, and k_s [20], and further, the relative values of the surface and bulk susceptibility components. The experimental results, together with the fitting curves, are shown in Figure 3. The fitting parameters normalized to $k_s = 1$ are $f_p = -0.680\pm0.018$, $g_p = -0.082\pm0.020$, and $h_s = -1.433\pm0.021$. The relative values of the corresponding susceptibility components are indicated in Table 1.
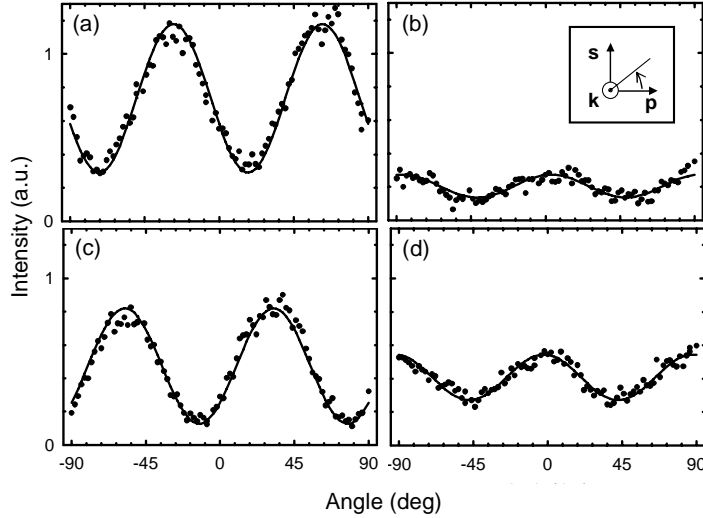

Fig. 3. Intensity of the SHG as a function of the angle of the quarter-wave plate in beam *b* for the combinations of the polarizations of the fundamental beam *a* and the detected SHG light: (a) 45°/90°, (b) 45°/0°, (c) 0°/45°, and (d) 90°/45°. The angles are defined like in the inset. The solid lines correspond to the fits with Eq. (10).

Table 1. Relative values of the susceptibility components.

χ_{xxz}^{sf}	1
$\chi_{zxx}^{sf} + \gamma$	0.49 ± 0.12
$\chi_{zzz}^{sf} + \gamma$	6.40 ± 0.91
δ'	1.01 ± 0.03

The error limits are calculated from the experimental noise at detection.

4. Discussion

The results of Table 1 suggest a straightforward but surprising interpretation of the origin of the bulk nonlinearity. If the effective surface susceptibility is assumed to fulfill Kleinman symmetry [15] so that $\chi_{xxz}^{sf} = \chi_{zxx}^{sf}$, we find that the relative value of the inseparable bulk contribution is about -0.5, i.e., that $\gamma \approx -0.5\delta'$. This result is exactly the one expected on

theoretical grounds if the bulk contribution has magnetic-dipole, rather than electric-quadrupole, character [14-16].

However, the validity of Kleinman symmetry for the effective surface susceptibility can be challenged for several reasons. First, the symmetry is valid only for the electric-dipole nonlinearity under strictly nonresonant conditions, i.e., when all optical frequencies are very much smaller than any of the resonance frequencies of the material, which is difficult to achieve in real experiments [21]. In addition, we see no reason to assume that the symmetry would be valid when the multipole contributions to the effective surface susceptibility are taken into account. We also note that, under strictly nonresonant conditions which validate Kleinman symmetry, the bulk parameter δ' vanishes because of symmetry reasons [3]. The experimental results clearly show that this is not true.

Nevertheless, there are also arguments that support approximate Kleinman symmetry of the effective surface nonlinearity. Ref. 21 has provided evidence that the surface nonlinearity of an air-water interface can be fully explained within the electric-dipole approximation with no need to consider multipole contributions. The importance of dipolar surface nonlinearity for an air-glass interface could also be much higher than previously thought [5]. Furthermore, we estimate on the basis of a quantum-mechanical expression that Kleinman symmetry of the dipolar surface susceptibility [22] is not violated by more than 30% in our experiment.

We have also considered the possibility of electric-quadrupole origin of the effective bulk nonlinearity. If the quadrupole interaction occurs at the fundamental frequency, the relative values of the two bulk parameters are $\gamma = 0.5\delta'$ [14-16,24]. When quadrupole effects at the second-harmonic frequency are taken into account, no strict relation between the bulk parameters can be found, but the same result should still be approximately valid. In our case, this limit would imply that $\chi_{zxx}^{sf} \approx 0$, which violates Kleinman symmetry very strongly and therefore appears coincidental and unlikely.

The above analysis therefore suggests that the magnetic contributions account for a significant fraction of the bulk nonlinearity of our glass sample. This is quite surprising, because BK7 does not include significant magnetic impurities. On the other hand, certain magnetic effects have been shown to be stronger than expected in several glasses including BK7 [23]. We also note that the bulk nonlinearity of C_{60}, although a very different material, has been shown to have magnetic-dipole origin [24]. And a very recent paper points towards the possibility of a much larger magnetic response at optical frequencies in dielectric materials than usually expected [25].

5. Conclusions

We have performed a quantitative tensorial measurement of the effective surface nonlinearity and the separable bulk nonlinearity of BK7 glass. The most straightforward, self-consistent interpretation of the results suggests a predominance of magnetic effects in the bulk response and relative unimportance of surface multipolar contributions. It is evident that further work including other materials will be necessary to investigate the universality of this result.

Acknowledgments